

Modest increase in the C:N ratio of N-limited phytoplankton in the California Current in response to high CO₂

Jenna L. Losh^{1,*}, Francois M. M. Morel¹, Brian M. Hopkinson^{1,2}

¹Department of Geosciences, Princeton University, Princeton, New Jersey 08544, USA

²Present address: Department of Marine Sciences, University of Georgia, Athens, Georgia 30602, USA

ABSTRACT: In a fall 2008 cruise off the coast of California, on-deck incubations with surface seawater were conducted to compare the effect of increasing carbon dioxide (CO₂) on nitrogen (N)-limited versus N-replete (+ NO₃⁻) phytoplankton. Based on previous laboratory studies, we expected that under N-limitation C:N ratios would be more sensitive to CO₂ availability. In particular, we wanted to test whether down-regulation of RuBisCO at high CO₂ leads to an increased C:N ratio, since RuBisCO is thought to be a large pool of N in many autotrophs. In 4 out of 5 N-limited experiments, the C:N ratio of phytoplankton biomass increased slightly from low to high CO₂, and this increase was due chiefly to an increase in particulate organic carbon (POC), with little change in particulate organic nitrogen (PON). In contrast, the N-replete experiments did not show a change in C:N ratio, but some experiments exhibited higher rates of carbon fixation and growth at high CO₂. In the one N-limited experiment that did not show a change in C:N ratio with CO₂, the ambient population had a higher proportion of cyanobacteria compared with the other experiments. The concentration of RuBisCO decreased at high CO₂ in several N-limited experiments, but this reduction only accounted for a minor proportion of the overall change in C:N ratio. An increase in C:N ratios at high CO₂ in N-limited phytoplankton could provide negative feedback to increasing atmospheric CO₂.

KEY WORDS: CO₂ · Phytoplankton · C:N ratios · N-limitation · RuBisCO

Resale or republication not permitted without written consent of the publisher

INTRODUCTION

Of the manifold possible consequences of the ongoing CO₂ increase in surface seawater, one of the most intriguing is that of increased primary production at elevated CO₂ levels. Such an effect could result in a negative feedback if it augmented the efficiency of the biological CO₂ pump. An increase in ambient CO₂ may be expected to alleviate the material and energetic demand of the carbon-concentrating mechanism of phytoplankton and result in faster growth rates, as has been reported in some studies (Rost et al. 2003, Tortell et al. 2008a, Hopkinson et al. 2011). A higher carbon fixation or growth rate at high

CO₂ has indeed been seen in some, though not all, field and laboratory experiments (Riebesell et al. 1993, Hein & Sand-Jensen 1997). But, by themselves, changes in growth rate do not affect the storage of CO₂ in deep seawater that results from the photosynthetic production and subsequent export of organic matter from the surface. In the large regions of the oceans that are limited by nitrogen (N), the export of organic carbon is effectively determined by the supply of new nitrogen to the surface and the C:N ratio of the sinking biomass. If nitrogen inputs to such regions remain the same, a change in CO₂ storage is only possible if the C:N ratio of the biomass changes. This could provide negative feedback to the ongoing

*Email: jlosh@princeton.edu

increase in atmospheric CO₂ if the additional carbon is not remineralized in the upper water column.

Previous laboratory studies with diatoms have reported species- and condition-specific trends, but no systematic differences, in C:N ratios over a range of CO₂ concentrations under nutrient-replete conditions (Burkhardt & Riebesell 1997, Burkhardt et al. 1999). No effect of CO₂ on the C:N ratio was seen in cultures of nutrient-replete cyanobacteria or in the coccolithophore *Emiliana huxleyi* (Barcelos e Ramos et al. 2007, Fu et al. 2007, 2008, Hutchins et al. 2007, Levitan et al. 2007, Feng et al. 2008, Iglesias-Rodriguez et al. 2008, Kranz et al. 2009). A similar absence of effect was seen with N-replete natural phytoplankton populations in bottle incubations and mesocosm experiments (Tortell et al. 2000, Kim et al. 2006, Feng et al. 2009, 2010).

Two previous experiments under N-limiting conditions provide background for our study. In a field mesocosm experiment in which nitrogen became limiting at the end of the simulated bloom, the ratio of dissolved inorganic carbon (DIC) to nitrate (NO₃⁻) drawdown increased from 6 to 8 at high CO₂, although the C:N ratio of the particulate matter did not change (Riebesell et al. 2007). A continuous culture experiment in the laboratory showed an increase in C:N ratio at high CO₂ under conditions of N limitation and high light in *Emiliana huxleyi* (Leonardos & Geider 2005). Such effects may result, for example, from an increase in carbon storage compounds (e.g. carbohydrates and lipids) or from a decrease in the cellular protein content. In particular, one may expect a down-regulation of the enzyme RuBisCO (1,5-ribulosebiphosphate carboxylase/oxygenase), which is thought to be an abundant enzyme and is undersaturated at ambient CO₂ concentrations (Badger et al. 1998). In the field, a change in the C:N stoichiometry of the biomass may also result from a change in phytoplankton community composition.

Here we report a field study designed to investigate the effect of CO₂ on the C:N stoichiometry of natural phytoplankton assemblages grown under N-limited and N-replete conditions off the coast of California. We hypothesized that C:N may increase at high CO₂ under N limitation, and sought to explore a decrease in the concentration of RuBisCO as a possible mechanism for any observed changes in C:N.

MATERIALS AND METHODS

Oceanographic context

We conducted 5 experiments off southern California in the Point Conception upwelling region and downstream as part of a Lagrangian study of biological processes in the California Current system (for earlier studies in this project, see Landry et al. 2009). The cruise was in the fall when upwelling is weak though still occurring, and only in Expt 4 was NO₃⁻ detectable in surface waters. The region is complex, as high productivity water from the upwelling region flows, ages, and mixes with oligotrophic offshore waters. Expts 1, 2, and 5 were initiated in lower productivity waters, while water for Expts 3 and 4 was collected from higher chlorophyll water masses, presumably more influenced by upwelling.

Experimental design

Over a period of 2 wk (15 to 27 October 2008), we conducted 5 incubation experiments lasting 3 to 4 d, varying in CO₂ and NO₃⁻ concentrations (Table 1). In all experiments, phosphorus, silicic acid, and iron were added. In the N-limited treatments, no NO₃⁻ was added, while the N-replete treatments received 10 or 20 μM NO₃⁻. Within each nitrogen treatment, we had 3 CO₂ treatments, nominally ½ atmospheric

Table 1. Sampling locations, initial nutrient concentrations, and calculated CO₂ concentrations from the beginning (t_0) and end (t_f) of the experiments. Data shown are from the N-replete treatments, where CO₂ concentrations changed the most due to carbon fixation. Data are means ± SD (n = 3). Bd: below detection level of 0.05 μM. Int.: intermediate

Expt	Latitude (°N)	Longitude (°W)	NO ₃ ⁻ initial (μM)	PO ₄ ³⁻ initial (μM)	Si initial (μM)	Low CO ₂ t_0 (μatm)	Low CO ₂ t_f (μatm)	Int. CO ₂ t_0 (μatm)	Int. CO ₂ t_f (μatm)	High CO ₂ t_0 (μatm)	High CO ₂ t_f (μatm)
1	33.97	121.78	bd	bd	2.3	204 ± 8	167 ± 9	365 ± 5	286 ± 4	884 ± 41	561 ± 24
2	34.19	121.64	bd	bd	1.8	235 ± 4	192 ± 3	361 ± 5	300 ± 0	834 ± 40	606 ± 17
3	33.64	121.18	bd	0.1	1.1	176 ± 3	153 ± 11	273 ± 4	244 ± 6	564 ± 35	421 ± 38
4	32.87	120.93	2.3	0.1	2.2	214 ± 9	192 ± 8	355 ± 5	335 ± 14	726 ± 17	599 ± 29
5	32.67	120.72	bd	0.1	2.2	185 ± 0	180 ± 0	307 ± 4	294 ± 7	622 ± 32	732 ± 27

CO₂, atmospheric CO₂, and 2× atmospheric CO₂, although the exact values differ somewhat, as shown in Table 1. Seawater was collected off a conductivity, temperature, depth (CTD) rosette cast from 10 to 20 m depth. Seawater was transferred directly to acid-washed 4 l polycarbonate bottles (Expt 1, Expt 2 N-limited, Expt 3, Expt 4, Expt 5 N-limited) or 4 l low-density polyethylene cubitators (Expt 2 N-replete, Expt 5 N-replete). Each experiment consisted of 18 bottles, 9 N-limited and 9 N-replete. Each set of 9 contained low, intermediate, and high CO₂ bottles in triplicate (described below). After CO₂ and nutrient manipulations, bottles were placed in on-deck incubators for 3 to 4 d with flow-through seawater (~16°C) at 20% surface irradiance controlled by neutral density screening.

CO₂ and nutrient manipulations

The target CO₂ values of the treatments aimed to approximate glacial ocean conditions, ambient ocean conditions, and atmospheric CO₂ to be reached in the next 100 yr in the low, intermediate, and high CO₂ bottles, respectively (Table 1). For the low pH/high CO₂ treatments, pH was reduced to ~7.8 using equimolar additions of HCl and NaHCO₃ (10% HCl, 1 M NaHCO₃, Sigma-Aldrich) with no associated change in alkalinity. In high pH/low CO₂ treatments, pH was adjusted to ~8.35 with NaOH (1 M NaOH, Sigma-Aldrich) with an approximate 150 to 200 μM increase in alkalinity. In experiments with lower biomass and where non-calcifying organisms are important, HCl/NaOH addition works well to control CO₂ (Shi et al. 2009). For ambient/intermediate CO₂ levels, collected seawater was used without adjustment. pH was measured daily using a pH electrode (Accumet Portable AP61 pH meter with an Accumet 55500-10 probe) calibrated before each use with standard NBS pH buffers (Fisher Scientific). pH values obtained with the pH meter were converted to the total hydrogen ion scale, pH_T, by intercalibration with measurements of pH_T using Thymol Blue (Zhang & Byrne 1996). In Expts 3 and 4, where initial biomass was relatively high, and in Expt 5, where the high-CO₂ bottles had not initially received sufficient acid, additional acid or base was added to the bottles once during the course of the experiment to maintain target CO₂ concentrations. In these cases, equimolar amounts of NaHCO₃ were again added to restore alkalinity. A volume of 25 ml of seawater was preserved with HgCl₂ in a glass vial at the beginning of each experiment for DIC analysis. DIC samples were

analyzed at the University of Georgia in the Cai laboratory through acid stripping of CO₂ followed by infrared measurements of CO₂ as described previously (Wang & Cai 2004). CO₂ concentrations were calculated based on pH, DIC, salinity (35 psu), and incubation temperature (16°C) using equilibrium constants from Dickson & Goyet (1994), with updates to the carbonic acid equilibria, on the pH_T scale, from Lueker et al. (2000).

To all bottles, 1.0 μM phosphorus, 14 μM silicate, and 2 nM iron were added. The N-replete bottles received 10 μM NO₃⁻ (Expts 1, 2, and 5) or 20 μM NO₃⁻ (Expts 3 and 4) depending on the initial chlorophyll values, while the N-limited bottles received no supplemental NO₃⁻. At *t* = 0 and final conditions for each bottle, 40 ml was filtered (0.2 μm filter) and frozen for nutrient analysis, including ammonium, silicate, phosphate, and nitrate and nitrite. Nutrient samples were submitted to the Woods Hole Nutrient Analytical Facility (Woods Hole, MA, USA) (Parsons et al. 1984).

Chlorophyll

At *t* = 0 and daily for each bottle, 50 to 200 ml water was filtered onto a glass fiber filter (GF/F, 25 mm, Whatman) and extracted in 7 ml 90% acetone, 10% water overnight in a freezer. Fluorescence was measured on a Turner 10-AU fluorometer before and after acidification and converted to μg l⁻¹ chlorophyll *a* (chl *a*) (Strickland & Parsons 1972). A net growth rate was calculated using the natural log of the ratio of the final to initial chlorophyll values over the duration of the experiments (Table 2).

Photosynthetic efficiency

At *t* = 0 and daily for each bottle, subsamples were collected to measure the kinetics of chlorophyll fluorescence induction and decay on a fluorescence induction and relaxation fluorometer (Satlantic). Samples were first acclimated in the dark for 15 to 45 min prior to measurement. In the single turnover phase, actinic blue light was applied for 80 μs to allow fluorescence to rise from its initial value (*F*₀) to its peak value (*F*_m) as the Photosystem II (PSII) reaction centers close. Relaxation was then monitored for 135 ms. A blank composed of 0.22 μm filtered sample was measuring using the same protocol, and this value was subtracted from the experimental data. The fluorescence response was then fitted to the

Table 2. Carbon fixation (CF; $\mu\text{mol C l}^{-1} \text{ h}^{-1}$), carbon fixation normalized to biomass (chl *a*) (CF^{B} ; $\mu\text{mol C } \mu\text{g chl } a^{-1} \text{ h}^{-1}$), intrinsic growth rate (μ_{POC} ; d^{-1}), net growth rate (μ_{chl} ; d^{-1}), and photosynthetic efficiency for 5 experiments. Data are means \pm SD ($n = 3$). nd, no data, carbon fixation measurements were not made on Expt 5. F_v/F_m values shown are averages from the daily measurements over the course of the experiments (for N-replete treatments, averages from exponential growth period)

Expt	Nutrient treatment	CO ₂ treatment	CF	CF ^B	μ_{POC}	μ_{chl}	F_v/F_m
1	N-limited	Low	0.24 \pm 0.01	0.39 \pm 0.13	0.19 \pm 0.01	-0.07 \pm 0.09	0.36 \pm 0.07
		Intermediate	0.25 \pm 0.02	0.41 \pm 0.10	0.18 \pm 0.03	-0.08 \pm 0.05	0.35 \pm 0.07
		High	0.23 \pm 0.03	0.37 \pm 0.01	0.13 \pm 0.01 ^{b,d}	-0.08 \pm 0.04	0.35 \pm 0.07
1	N-replete	Low	1.6 \pm 0.14	0.31 \pm 0.02 ^a	0.66 \pm 0.16	0.56 \pm 0.02 ^a	0.36 \pm 0.06
		Intermediate	1.4 \pm 0.21	0.36 \pm 0.03	0.69 \pm 0.10	0.46 \pm 0.07	0.37 \pm 0.05
		High	2.3 \pm 0.21 ^{c,d}	0.37 \pm 0.05	0.90 \pm 0.11	0.62 \pm 0.01 ^{a,d}	0.47 \pm 0.05
2	N-limited	Low	0.12 \pm 0.02	0.43 \pm 0.05	0.13 \pm 0.02	-0.22 \pm 0.02	0.30 \pm 0.03
		Intermediate	0.14 \pm 0.02	0.57 \pm 0.05	0.14 \pm 0.02	-0.25 \pm 0.04	0.29 \pm 0.02
		High	0.13 \pm 0.04	0.58 \pm 0.19	0.12 \pm 0.03	-0.27 \pm 0.02	0.25 \pm 0.08
2	N-replete	Low	1.1 \pm 0.06 ^b	0.32 \pm 0.03	0.42 \pm 0.07	0.50 \pm 0.02 ^c	0.37 \pm 0.04
		Intermediate	0.86 \pm 0.10	0.36 \pm 0.02	0.41 \pm 0.01	0.40 \pm 0.02	0.36 \pm 0.05
		High	1.4 \pm 0.11 ^{c,d}	0.41 \pm 0.01 ^{b,d}	0.70 \pm 0.09 ^{b,d}	0.51 \pm 0.03 ^b	0.37 \pm 0.05
3	N-limited	Low	0.35 \pm 0.12	0.36 \pm 0.033	0.15 \pm 0.05	-0.13 \pm 0.08	0.38 \pm 0.04
		Intermediate	0.29 \pm 0.01	0.36 \pm 0.05	0.11 \pm 0.01	-0.14 \pm 0.04	0.36 \pm 0.06
		High	0.27 \pm 0.03	0.36 \pm 0.06	0.10 \pm 0.02	-0.20 \pm 0.04	0.38 \pm 0.03
3	N-replete	Low	4.2 \pm 1.0	0.32 \pm 0.03	0.75 \pm 0.05 ^b	0.95 \pm 0.14	0.39 \pm 0.11
		Intermediate	4.5 \pm 1.1	0.37 \pm 0.03	0.88 \pm 0.03	0.91 \pm 0.06	0.36 \pm 0.07
		High	7.4 \pm 0.9 ^{b,d}	0.54 \pm 0.10 ^{a,d}	1.1 \pm 0.10 ^d	0.98 \pm 0.08	0.38 \pm 0.14
4	N-limited	Low	0.90 \pm 0.06	0.26 \pm 0.03	0.18 \pm 0.02 ^a	0.12 \pm 0.05	0.43 \pm 0.07
		Intermediate	0.89 \pm 0.17	0.30 \pm 0.43	0.20 \pm 0.03	0.02 \pm 0.05	0.44 \pm 0.06
		High	0.67 \pm 0.10 ^d	0.21 \pm 0.04	0.12 \pm 0.03 ^b	0.08 \pm 0.01	0.44 \pm 0.09
4	N-replete	Low	2.9 \pm 0.41	0.27 \pm 0.04	0.44 \pm 0.07	0.59 \pm 0.05	0.44 \pm 0.03
		Intermediate	2.6 \pm 0.11	0.25 \pm 0.02	0.25 \pm 0.02	0.56 \pm 0.02	0.42 \pm 0.03
		High	3.2 \pm 0.22 ^b	0.28 \pm 0.03	0.28 \pm 0.03	0.60 \pm 0.02 ^a	0.43 \pm 0.05
5	N-limited	Low	nd	nd	nd	-0.52 \pm 0.37	0.42 \pm 0.03
		Intermediate	nd	nd	nd	-0.52 \pm 0.18	0.40 \pm 0.03
		High	nd	nd	nd	-0.48 \pm 0.30	0.40 \pm 0.05
5	N-replete	Low	nd	nd	nd	0.77 \pm 0.10	0.42 \pm 0.04
		Intermediate	nd	nd	nd	0.71 \pm 0.15	0.39 \pm 0.03
		High	nd	nd	nd	0.84 \pm 0.08	0.40 \pm 0.06

^aSignificantly different from intermediate CO₂, $p < 0.1$; ^bsignificantly different from intermediate CO₂, $p < 0.05$;
^csignificantly different from intermediate CO₂, $p < 0.01$; ^dsignificantly different from low CO₂, $p < 0.1$

Kolber et al. (1998) model of variable fluorescence to yield F_0 and F_m . Maximum quantum yield (F_v/F_m) was calculated as $(F_m - F_0)/F_m$.

Carbon fixation and growth rates

On the final day of Expts 1 to 4, 2.5 to 5 μCi inorganic ¹⁴C was added to 40 ml from each of the 18 bottles and incubated for 2 to 3 h in acid-cleaned polycarbonate bottles in the same screened flow-through incubators in which the experiments were conducted. Productivity measurements were not taken in Expt 5. The water was filtered through a GF/F filter, which was then placed in a scintillation vial. One milliliter of 2% HCl was added to the scintillation vial and the vial was allowed to degas overnight to

remove inorganic carbon. A sample (0.5 ml unfiltered water, to which 0.5 ml β -phenethylamine was added) was also taken for analysis of total ¹⁴C activity. Scintillation fluid (ScintSafe Plus 50%, Fisher Scientific) was added to the samples and ¹⁴C content was determined by liquid scintillation counting. Gross carbon fixation (CF) rates ($\mu\text{mol C l}^{-1} \text{ h}^{-1}$) were determined assuming that the rate of fixation was linear over the time of experiment, and using measured DIC (Table 2). These data, combined with particulate organic carbon data ($\mu\text{mol C l}^{-1}$, described below), were used to estimate the intrinsic phytoplankton growth rates ($\mu_{\text{POC}} = \text{CF POC}^{-1}$). Carbon fixation normalized to chl *a* biomass (CF^{B} ; $\mu\text{mol } \mu\text{g chl } a^{-1} \text{ l}^{-1}$) was calculated by dividing the gross carbon fixation rates by the chlorophyll data taken on the final day of each experiment.

Elemental stoichiometry

At $t = 0$ and the final time point for each bottle, varying amounts of water (~1 l) were filtered onto a precombusted GF/F filter. The filters were stored in liquid N₂ for the duration of the cruise and transport, and then at -80°C. For analysis, ¼ or ½ of each filter was dried overnight at 60°C, exposed to fuming HCl for 6 h to remove any calcium carbonate, and dried overnight again at 60°C. Samples were packed in tin cups (Costech Analytical Technologies) and measured on an elemental analyzer coupled to an isotope ratio mass spectrometer (e.g. Orcutt et al. 2001). C:N ratios were calculated on a mole-to-mole basis based on micrograms of particulate organic carbon (POC) and micrograms of particulate organic nitrogen (PON).

Photosynthetic proteins

At $t = 0$ and the final time point for each bottle, ~2 l water was filtered through a 0.22-µm Sterivex filter cartridge using a peristaltic pump. Samples were flash-frozen in liquid N₂ and stored at -80°C until processing. Total protein concentration was determined using the BCA protein assay (Pierce, Thermo Scientific) as described in Hopkinson et al. (2010). Western blots were performed to quantify proteins of interest (e.g. McGinn & Morel 2008) including RbcL, the large subunit of RuBisCO, and PsbA, also known as D1, a core reaction center protein in PSII. Equal amounts of total protein (1 or 2 µg) were loaded on 12% or 15% SDS-PAGE gels and run for 35 to 45 min at 250 V in 1× sodium dodecyl sulfate running buffer. A series of 3 or 4 RbcL or PsbA standards (Agriser) were run alongside experimental protein samples to generate a standard curve and determine the absolute protein concentration of each sample. Results were only used when samples fell within the linear range of loaded standards. After electrophoresis, proteins were transferred to a polyvinylidene fluoride membrane in ice-cold Tris/glycine transfer buffer for 2 h at 200 mA. The membrane was then blocked with Tris-buffered saline/Tween 20 (TBST)-milk buffer for 1 h at room temperature on a shaker. The primary antibodies for RbcL and PsbA were raised in rabbit and are both polyclonal, global antibodies (Agriser) designed against peptide tags that are conserved across all oxygenic photosynthesizers so that no bias in affinity is expected even if phytoplankton communities differ (Campbell et al. 2003). One microliter of the primary antibody (1:10 000 dilution) and 2 µl of the secondary

antibody (1:5000 dilution, alkaline phosphate-coupled goat anti-rabbit IgG antibody, Pierce) was used, followed by three 5-min washes and then two 10-min washes in TBST-milk buffer. Protein bands were visualized by either colorimetric analysis, by quickly washing twice with PhoA buffer and then adding 0.5% nitro-blue tetrazolium chloride/5-bromo-4-chloro-3-indolylphosphate *p*-toluidine (NBT/BCIP) in PhoA buffer for 5 to 10 min, or by more sensitive chemiluminescent detection. For the latter, the membrane was submersed in 3 ml Immobilon western chemiluminescent AP substrate (Millipore) for 3 min, and then placed in plastic wrap. The membrane was exposed to clear blue X-ray film (Thermo Scientific) in a hypercassette (Amersham Biosciences) for an appropriate exposure time (between 3 s and 3 min), and then developed in an X-ray machine (Kodak 2100A). Results were normalized to total protein by directly comparing the intensities of the bands on the Western blot using ImageJ, a public domain image processing program.

Taxonomic pigments

The remaining portion of the GF/F filter from elemental stoichiometry analysis was used to quantify taxonomically informative phytoplankton pigments. Pigments were analyzed by HPLC using a modified version of the method described in Goericke & Montoya (1998). Filters were extracted on ice in 1.5 ml acetone for 0.5 h, homogenized, and allowed to extract for a further 0.5 h. Following centrifugation, portions of the extract were mixed with water to produce a 60:40 acetone:water solution, and immediately injected in the HPLC system. Pigments were then separated on a 10 cm Supelco Discovery BIO Wide Pore C8 column, using a gradient between methanol:0.5 mol l⁻¹ aqueous ammonium acetate (75:25) and methanol. Chromatographic peaks were identified by retention time, and quantified by peak area using calibrations determined from pure pigments isolated from algal cultures.

Statistics

Differences between nitrogen and CO₂ treatments were assessed using a 2-sample unequal variance *t*-test with 2 tails. For each parameter tested (e.g. POC, D1 protein), triplicate data from the low and high CO₂ treatments were compared with the reference treatment, intermediate CO₂. To test for significance

for key parameters of interest across all experiments (C:N, POC, RbcL), triplicate data within each experiment were normalized to the mean of a reference CO₂ treatment—for example, Expt 1 low CO₂ when comparing Expt 1 intermediate with Expt 1 high CO₂. Normalized values were then pooled from all 5 experiments and compared as described above using a *t*-test.

RESULTS AND DISCUSSION

Growth

The pH changed by less than 0.1 pH units in the bottles (as a result of the low biomass, or in 2 cases because of pH readjustment with equimolar acid/bicarbonate; see 'Materials and methods') so that the 3 CO₂ treatments remained distinct from each other throughout the course of the experiments (Table 1). At all but one station, the treatments with no N addition were limited by N at the onset (initial NO₃⁻ < 0.05 μM). In Expt 4, which had an initial NO₃⁻ concentration of 2.3 μM, all N was consumed by the end of the experiment. We refer to all of these as N-limited treatments (Table 1). As expected, the addition of phosphate, silicic acid, and iron did not stimulate growth in any N-limited treatments (Fig. 1). Final time point nutrient data confirmed N-replete conditions in the N-amended bottles with at least 3 μM NO₃⁻ remaining, as well as sufficient residual Si and PO₄³⁻ in all bottles (data not shown).

As expected, addition of NO₃⁻ stimulated phytoplankton growth over the N-limited treatments in all experiments as seen in daily chl *a* measurements (Fig. 1) and POC (Fig. 2). While the N-limited treatments did not show an increase in chl *a* over time, intrinsic growth rates (μ_{POC}) calculated from carbon fixation and POC confirmed the populations were turning over (Table 2) as a result of a balance between photosynthesis and respiration/grazing. Under N-replete conditions, high CO₂ generally increased chl *a* as well as the rates of carbon fixation and growth (Fig. 1, Table 2), in agreement with previous studies (Hein & Sand-Jensen 1997, Egge et al. 2009). No such trend was observed in the N-limited experiments.

Photosynthetic efficiency, as quantified daily by F_v/F_m measurements, did not show any trends between nitrogen or CO₂ treatments, as illustrated by the mean values shown in Table 2. This is somewhat surprising since F_v/F_m is known to decline under nitrogen starvation (e.g. Cleveland & Perry 1987,

Parkhill et al. 2001). However, it may reflect the acclimation of the ambient community to N-limiting conditions since F_v/F_m has been shown to remain high under N-limited balanced growth (Parkhill et al. 2001). Nevertheless, the dramatic phytoplankton growth after NO₃⁻ addition clearly shows there is a difference in the nitrogen status of the treatments.

Elemental stoichiometry

C:N ratios of the ambient particulate matter taken at the beginning of each experiment exceeded Redfield ratios in 4 out of 5 locations, ranging from 6.4 to 12.2 (Fig. 2C). The lowest initial C:N ratio, 6.4 in Expt 4, corresponds to the only location with detectable NO₃⁻ initially (Table 1). The other elevated initial C:N values likely reflect N limitation, as has been noted in other oligotrophic areas (Geider & La Roche 2002) and in numerous laboratory continuous culture experiments (e.g. Caperon & Meyer 1972, Goldman & Peavey 1979, Laws & Bannister 1980). Correspondingly, in Expts 1 to 4, the C:N ratios of the N-limited bottles were significantly higher than those in the N-replete bottles ($p < 0.05$; Fig. 2C).

Under conditions of N limitation in Expts 1 to 4, the C:N ratios increased systematically with increasing CO₂ (Fig. 2C), but the differences were only significant in 2 instances (between high and intermediate CO₂ in Expts 1 and 4, $p < 0.05$). The differences among treatments from low to intermediate and intermediate to high CO₂ become significant ($p < 0.05$) when the results from all 5 experiments are normalized and pooled together (see 'Materials and methods', and Fig. S1 in the supplement at www.int-res.com/articles/suppl/m468p031_supp.pdf). Most of the increase in C:N is attributable to an increase in POC with increasing CO₂, while the PON shows no systematic variation (Fig. 2A,B). Like the difference in C:N ratio, this difference in POC is only significant in Expt 1, but becomes significant for the ensemble when the data are normalized and pooled together ($p < 0.05$, Fig. S1 in the supplement). This increase in C:N and POC at high CO₂ is in accord with the laboratory results of Leonardos & Geider (2005) in N-limited continuous culture experiments.

As expected, POC and PON were significantly higher in the N-replete treatments compared with the N-limited treatments, regardless of CO₂ concentration, in all experiments ($p < 0.001$; Fig. 2A,B). But there was no change in the C:N ratio and no trend in POC or PON with increasing CO₂ in the N-replete treatments. These results are consistent with several

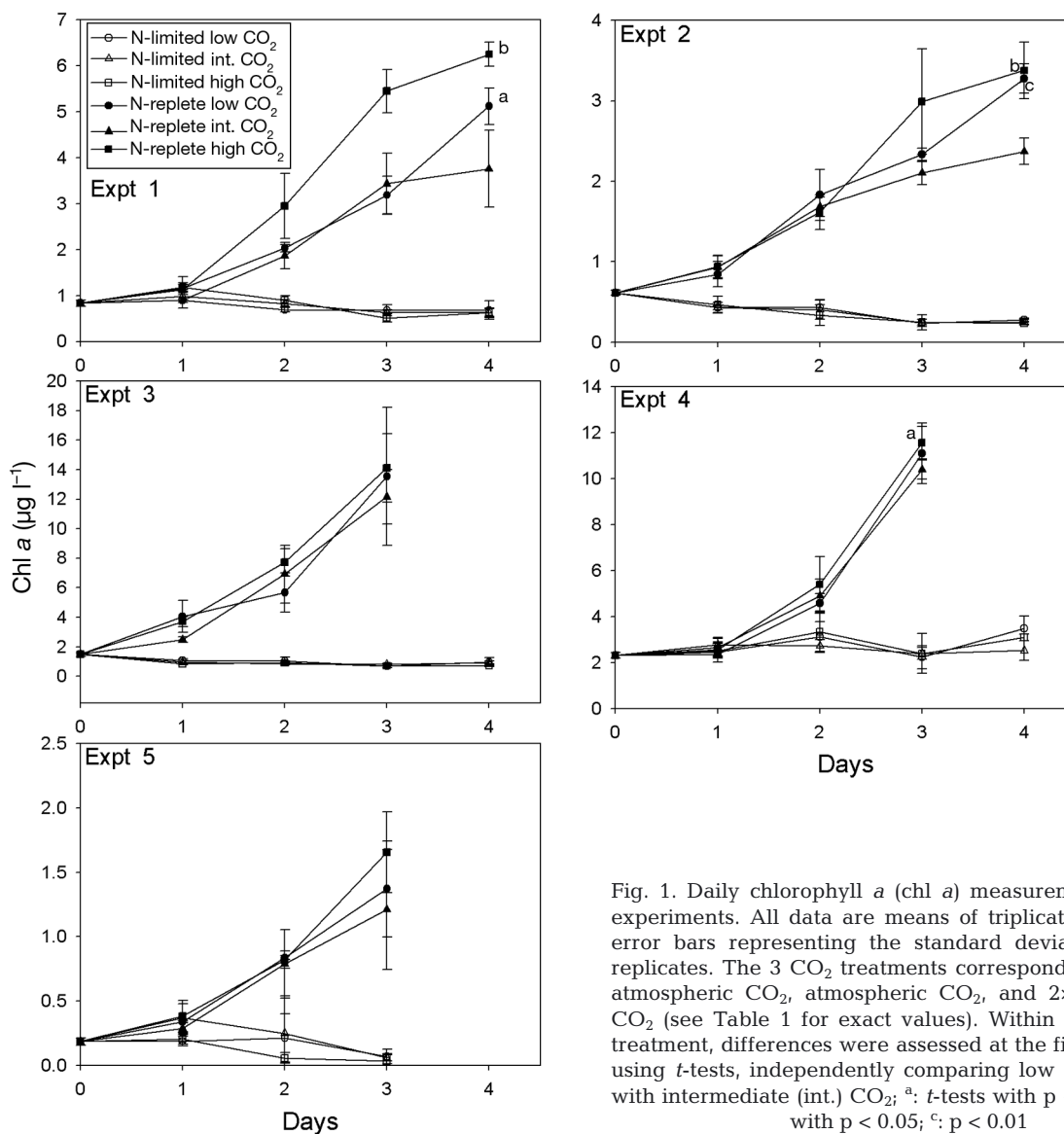


Fig. 1. Daily chlorophyll *a* (chl *a*) measurements from all experiments. All data are means of triplicate bottles with error bars representing the standard deviation between replicates. The 3 CO₂ treatments correspond roughly to ½ atmospheric CO₂, atmospheric CO₂, and 2× atmospheric CO₂ (see Table 1 for exact values). Within each nitrogen treatment, differences were assessed at the final time point using *t*-tests, independently comparing low and high CO₂ with intermediate (int.) CO₂; ^a: *t*-tests with *p* < 0.1; ^b: *t*-tests with *p* < 0.05; ^c: *p* < 0.01

field studies that have investigated the response of phytoplankton stoichiometric ratios to CO₂ and reported no change in C:N with CO₂ under nutrient-replete conditions (Tortell et al. 2000, Kim et al. 2006, Fu et al. 2007, 2008, Feng et al. 2009, 2010).

The results of Expt 5 differ from the others in 2 ways: (1) there was no difference in the C:N ratios between N-limited and N-replete treatments, and (2) there was no effect of CO₂ on the C:N ratio under N limitation. This may be explained by differences in community structure as discussed below, but it may also have been caused by the shorter duration of the experiment (less than 3 d).

The increase in C:N ratio we observed at high CO₂ in 4 of our N-limited experiments could be caused either by a change in the composition of the particu-

late material of the dominant species of phytoplankton, or by a shift in the taxa of the dominant species, or both. Both of these effects have been observed in various field and laboratory experiments under varying conditions and in different locations. In experiments where the C:N ratio of *Emiliana huxleyi* increased at high CO₂ under N-limitation and the POC/cell increased as well, the authors suggested an increase in cellular neutral lipids or carbohydrates to explain the trend (Leonardos & Geider 2005). Others have proposed an increase in transparent exopolymer particles (TEP) at high CO₂ to explain changes in C:N stoichiometry under nutrient stress (Engel 2002, Engel et al. 2004, Riebesell et al. 2007). These polymers, which are thought to form by aggregation of dissolved precursors and increase under N limitation,

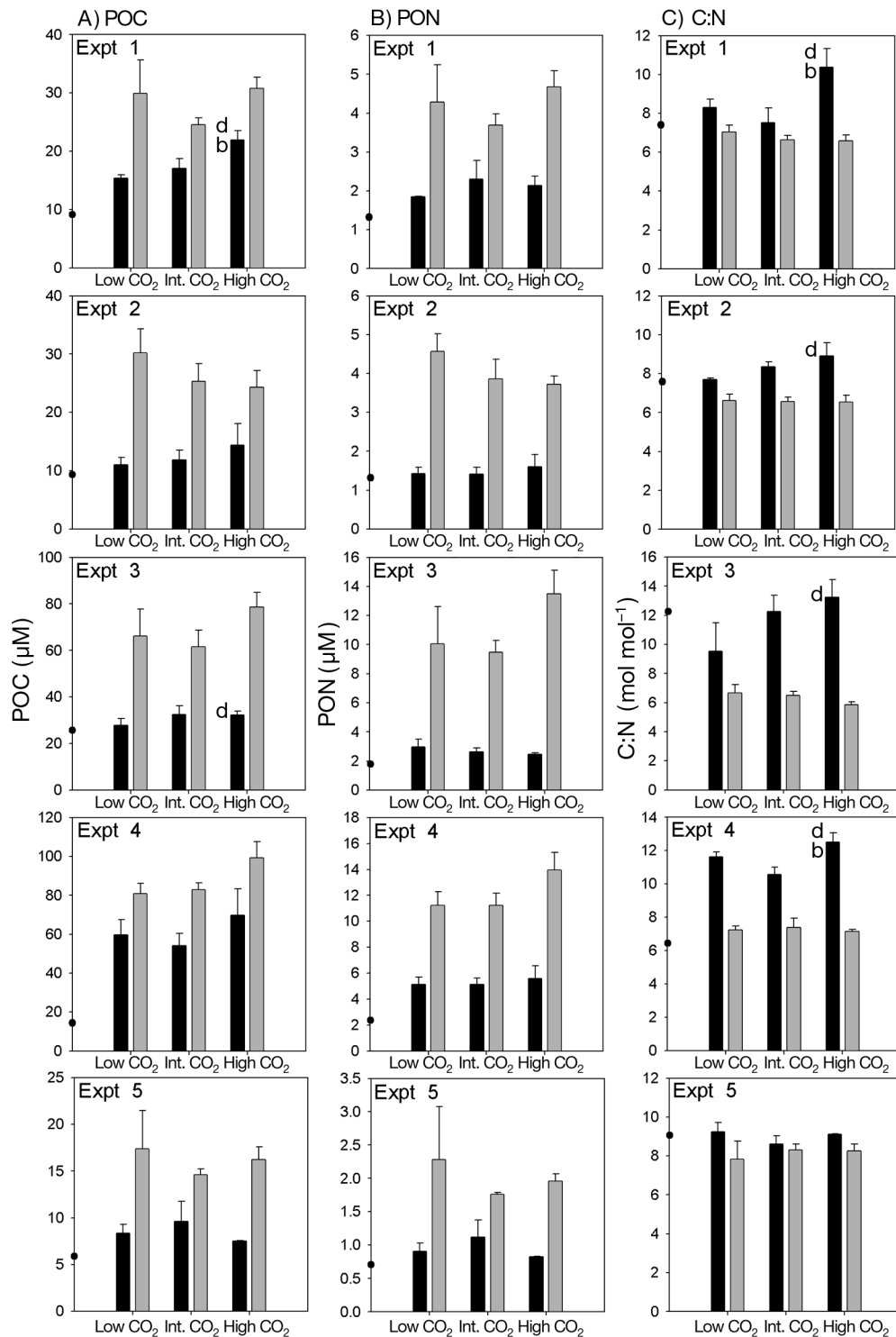


Fig. 2. (A) Particulate organic carbon (POC), (B) particulate organic nitrogen (PON), and (C) C:N data at the final time point from all experiments. Values are means of triplicate bottles with error bars representing the standard deviation between replicates, except for Expt 1 N-limited low CO₂, which are from 2 bottles. The black bars are N-limited treatments, the gray bars are the N-replete treatments, and the solid circles are the $t = 0$ values. The 3 CO₂ treatments correspond roughly to $\frac{1}{2}$ atmospheric CO₂, atmospheric CO₂, and $2 \times$ atmospheric CO₂ (see Table 1 for exact values). Within each nitrogen treatment, differences were assessed at the final time point using t -tests independently comparing low and high CO₂ with intermediate (int.) CO₂; ^b: t -tests with $p < 0.05$; ^d: t -tests directly comparing low and high CO₂ with $p < 0.1$.

are partly retained on filters and measured with the particulate material (Engel 2000).

Taxonomic pigments

Since different types of phytoplankton carry different C:N signatures, increasing CO₂ may have shifted the phytoplankton community towards those with higher C:N ratios (Finkel et al. 2010). We examined the community structure by pigment analysis at the beginning and end of each experiment. At $t = 0$, Expt 1 was dominated by prymnesiophytes (19-hex), Expts 2, 3, and 4 were dominated by both diatoms and prymnesiophytes (19-hex, fucox), and Expt 5 was dominated equally by prymnesiophytes and cyanobacteria (19-hex, zeax) (Fig. 3, Fig. S2 in the supplement). In all experiments, the phytoplankton assemblages at the end of the N-limited experiments were similar to those at the beginning, while addition of NO₃⁻ stimulated diatoms (fucox) over all other groups, with the exception of Expt 5. Importantly, in no experiments was there a significant effect of CO₂ on the community composition (Fig. 3, Fig. S2 in the supplement). The quite different floral composition of Expt 5, namely the importance of cyanobacteria, which must have been numerically dominant as evinced by the zeaxanthin concentration, may explain the different results that were obtained. Such differences may be caused by the composition of the phytoplankton itself or by the carbon and nitrogen cycling of the microbial community.

While some changes in community composition have been seen in other field incubations, for example increased phytoplankton productivity and increased growth of larger chain-forming diatoms at elevated CO₂ in incubations in the Ross Sea (Tortell et al. 2002 2008b), no shifts in the diatom- and prymnesiophyte-dominated phytoplankton community were induced by CO₂ in the Norway mesocosm experiments mentioned earlier (Riebesell et al. 2007).

Photosynthetic proteins

Because a high CO₂ concentration may decrease the requirements for proteins involved in inorganic carbon acquisition and fixation, it may result in lower protein content of the cell and hence a higher C:N ratio. The most important of these proteins is RuBisCO, which carries out the initial carboxylation reaction in photosynthesis and has been suggested to account for a large fraction of cellular protein in phytoplankton, as it does in some higher plants (Pickersgill 1986, Campbell et al. 1988). To test this possibility, we quantified total cellular protein as well as the absolute concentrations of RuBisCO and PsbA/D1 protein, a reaction center of PSII.

To cause a 2 unit (mol:mol) change in C:N ratio as seen in our N-limited experiments, the protein content of the cell must decrease by approximately 35% at high CO₂, assuming 50% of the carbon biomass is protein and that protein has a C:N ratio of 3.5 (Falkowski & Raven 2007). No systematic differences

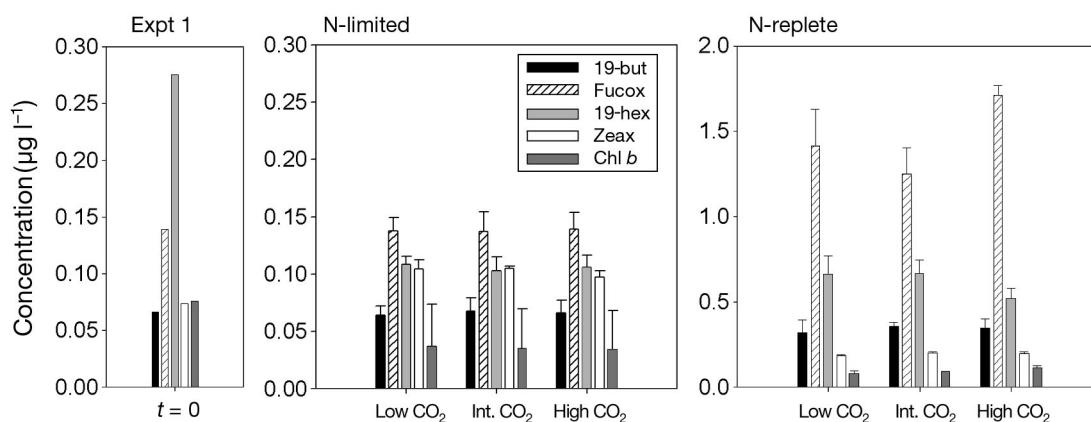


Fig. 3. Phytoplankton pigment concentrations at the initial and final time point of Expt 1. Pigments are derived from the following taxa: 19-butanoyloxyfucoxanthin (19-but): pelagophytes, prymnesiophytes; fucoxanthin (fucox): diatoms, prymnesiophytes; 19-hexanoyloxyfucoxanthin (19-hex): prymnesiophytes; zeaxanthin (zeax): cyanobacteria; chlorophyll *b* (chl *b*): chlorophytes. Pigments shown are the 5 highest in concentration across all experiments. Final time point data are means of triplicate bottles with error bars representing the standard deviation between replicates. Initial time point data are from a single sample. The 3 CO₂ treatments (low, intermediate [int.] and high) correspond roughly to ½ atmospheric CO₂, atmospheric CO₂, and 2× atmospheric CO₂, respectively (see Table 1 for exact values)

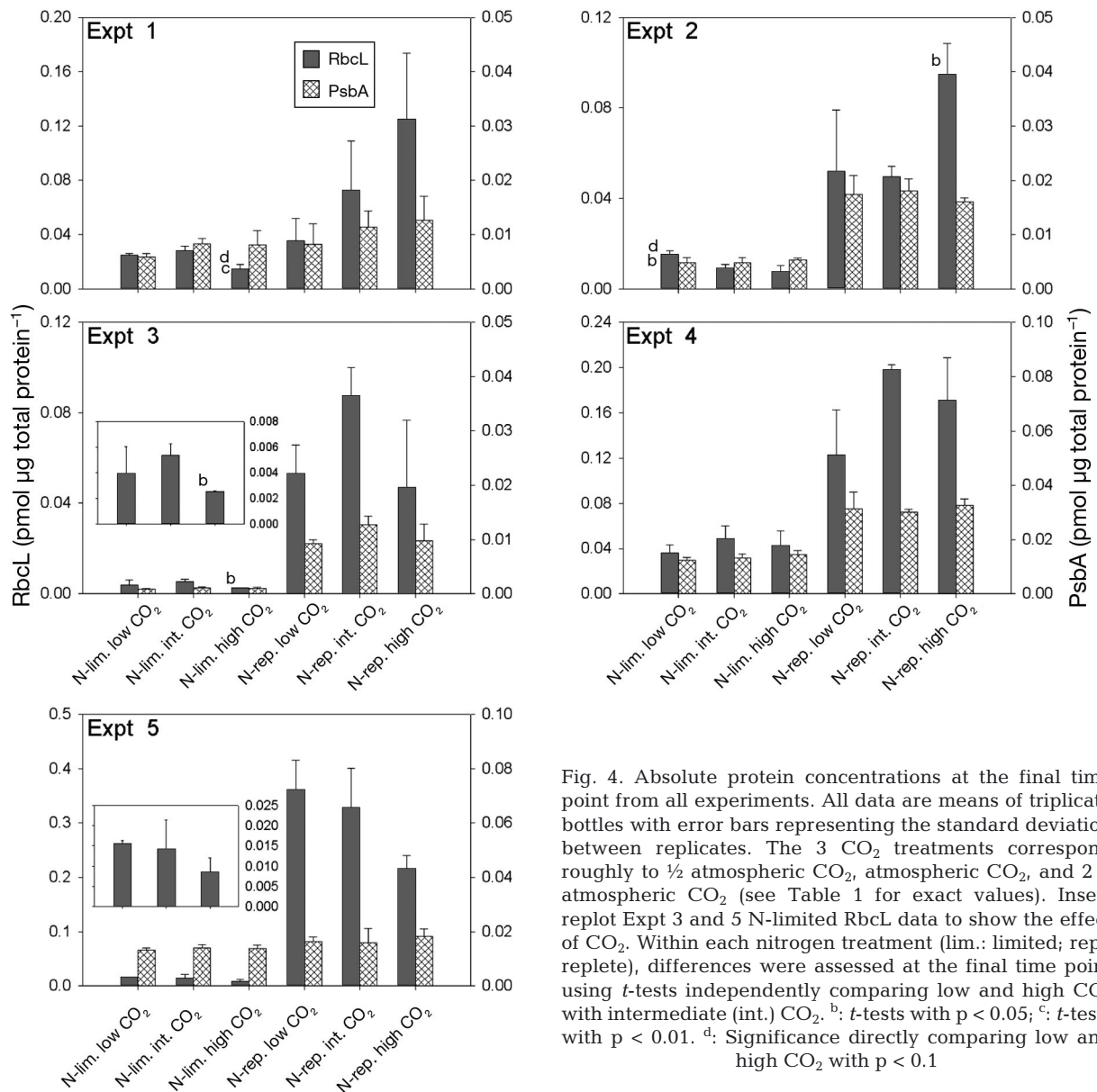


Fig. 4. Absolute protein concentrations at the final time point from all experiments. All data are means of triplicate bottles with error bars representing the standard deviation between replicates. The 3 CO₂ treatments correspond roughly to 1/2 atmospheric CO₂, atmospheric CO₂, and 2 × atmospheric CO₂ (see Table 1 for exact values). Insets replot Expt 3 and 5 N-limited RbcL data to show the effect of CO₂. Within each nitrogen treatment (lim.: limited; rep.: replete), differences were assessed at the final time point using *t*-tests independently comparing low and high CO₂ with intermediate (int.) CO₂. ^b: *t*-tests with *p* < 0.05; ^c: *t*-tests with *p* < 0.01. ^d: Significance directly comparing low and high CO₂ with *p* < 0.1

could be seen in total protein content due to CO₂ in either nitrogen treatment (Fig. S3 in the supplement). Our total protein measurements had an inherent variability of 15%, low enough to conclude that a decrease in total protein content cannot explain the increase in C:N ratio. There was a clear increase in total protein in the N-replete treatments by a factor of 2 to 3 over the N-limited treatments in all experiments (Fig. S3 in the supplement).

We compared the concentrations of 2 proteins, RuBisCO, which we expected to respond to CO₂, and PsbA/D1, which we did not expect to respond to CO₂. In all N-replete experiments, the absolute concentration (pmol protein µg total protein⁻¹) of RuBisCO and

PsbA/D1 protein exceeded that of the N-limited treatments by at least a factor of 3 (Fig. 4). But the concentration of neither of these proteins varied systematically with CO₂ across experiments, although increasing or decreasing trends were seen for RuBisCO in some experiments.

For the N-limited treatments in Expts 1, 2, 3, and 5, we saw no change in PsbA/D1, but an approximately 50% decrease in RuBisCO was seen at high CO₂, except in Expt 4 (Fig. 4). This change was only significant in 2 individual experiments, Expts 1 and 3 (*p* < 0.05), but became significant for the ensemble when the data were normalized and pooled together (see 'Materials and methods'; *p* < 0.05). This trend agrees

with our hypothesis that RuBisCO may be down-regulated at high CO₂. However, RuBisCO accounted for less than 5% of total protein (data not shown) in all experiments such that even a 50% decrease can only result in a 2.5% change in protein concentration, much less than the required 35% decrease. The fraction of total protein that RuBisCO accounted for in our experiments is within range of previous measurements of RuBisCO in microalgae (2 to 15%, Raven 1991). Consequently, the down-regulation of RuBisCO may contribute to the rise in C:N ratio at high CO₂, but accounts for at most a minor fraction of the overall change.

CONCLUSIONS

Our field data show that increasing CO₂ can result in a modest increase in the C:N ratio of the biomass produced by N-limited phytoplankton. This result was not seen in an experiment where cyanobacteria were numerically dominant, but was seen in 4 other experiments where diatoms and prymnesiophytes dominated the ambient biomass. This effect does not appear to be caused by shifts in community structure with CO₂, and so must result from a change in the elemental composition of the ambient phytoplankton. However, it is not caused by a decrease in the cellular concentration of total protein or RuBisCO, and so most likely is due to the production of C-rich material such as storage lipids, polysaccharides, or TEP. If such increases in C:N ratios in N-limited cells prove to occur generally, they might provide a negative feedback to the ongoing increase in atmospheric CO₂, provided the additional POC is not remineralized at the surface.

Acknowledgements. We appreciate the support of the science team and crew aboard the RV 'Melville' and the California Current Ecosystem Long-Term Ecological Response (CCE LTER) program, specifically Michael Landry (Scripps Institution of Oceanography [SIO]), Chief Scientist on the cruise, and Mark Ohman (SIO) for allowing us to participate in the cruise. We thank Linda Godfrey at Rutgers University for her help processing solid samples. This work is supported by the National Science Foundation and the Graduate Research Fellowship Program.

LITERATURE CITED

- Badger MR, Andrews TJ, Whitney SM, Ludwig M, Yellowlees DC, Leggat W, Price GD (1998) The diversity and coevolution of rubisco, plastids, pyrenoids, and chloroplast-based CO₂-concentrating mechanisms in algae. *Can J Botany* 76:1052–1071
- Barcelos e Ramos J, Biswas H, Schulz KG, LaRoche J, Riebesell U (2007) Effect of rising atmospheric carbon dioxide on the marine nitrogen fixer *Trichodesmium*. *Global Biogeochem Cycles* 21,GB2028, doi: 10.1029/2006GB002898
- Burkhardt S, Riebesell U (1997) CO₂ availability affects elemental composition (C:N:P) of the marine diatom *Skeletonema costatum*. *Mar Ecol Prog Ser* 155:67–76
- Burkhardt S, Zondervan I, Riebesell U (1999) Effect of CO₂ concentration on C:N:P ratio in marine phytoplankton: a species comparison. *Limnol Oceanogr* 44:683–690
- Campbell WJ, Allen LH, Bowes G (1988) Effects of CO₂ concentration on rubisco activity, amount, and photosynthesis in soybean leaves. *Plant Physiol* 88:1310–1316
- Campbell DA, Cockshutt AM, Porankiewicz-Asplund J (2003) Analysing photosynthetic complexes in uncharacterized species or mixed microalgal communities using global antibodies. *Physiol Plant* 119:322–327
- Caperon J, Meyer J (1972) Nitrogen-limited growth of marine phytoplankton. I. Changes in population characteristics with steady-state growth-rate. *Deep-Sea Res* 19:601–618
- Cleveland JS, Perry MJ (1987) Quantum yield, relative specific absorption and fluorescence in nitrogen-limited *Chaetoceros gracilis*. *Mar Biol* 94:489–497
- Dickson AG, Goyet C (eds) (1994) DOE handbook of methods for the analysis of the various parameters of the carbon dioxide system in sea water, 2nd edn. ORNL/CDIAC-74 (Carbon Dioxide Information Analysis Center, Oak Ridge National Laboratory), Oak Ridge, TN
- Egge JK, Thingstad TF, Larsen A, Engel A, Wohlers J, Bellerby RGJ, Riebesell U (2009) Primary production during nutrient-induced blooms at elevated CO₂ concentrations. *Biogeosciences* 6:877–885
- Engel A (2000) The role of transparent exopolymer particles (TEP) in the increase in apparent particle stickiness (alpha) during the decline of a diatom bloom. *J Plankton Res* 22:485–497
- Engel A (2002) Direct relationship between CO₂ uptake and transparent exopolymer particles production in natural phytoplankton. *J Plankton Res* 24:49–53
- Engel A, Delille B, Jacquet S, Riebesell U, Rochelle-Newall E, Terbruggen A, Zondervan I (2004) Transparent exopolymer particles and dissolved organic carbon production by *Emiliana huxleyi* exposed to different CO₂ concentrations: a mesocosm experiment. *Aquat Microb Ecol* 34:93–104
- Falkowski PG, Raven JA (2007) Aquatic photosynthesis. Princeton University Press, Princeton, NJ
- Feng Y, Warner ME, Zhang Y, Sun J, Fu F, Rose JM, Hutchins DA (2008) Interactive effects of increased pCO₂, temperature and irradiance on the marine coccolithophore *Emiliana huxleyi* (Prymnesiophyceae). *Eur J Phycol* 43:87–98
- Feng Y, Hare CE, Leblanc K, Rose JM and others (2009) Effects of increased pCO₂ and temperature on the north atlantic spring bloom. I. The phytoplankton community and biogeochemical response. *Mar Ecol Prog Ser* 388:13–25
- Feng Y, Hare CE, Rose JM, Handy SM and others (2010) Interactive effects of iron, irradiance and CO₂ on Ross Sea phytoplankton. *Deep-Sea Res Part I* 57:368–383
- Finkel ZV, Beardall J, Flynn KJ, Quigg A, Rees TAV, Raven JA (2010) Phytoplankton in a changing world: cell size and elemental stoichiometry. *J Plankton Res* 32:119–137
- Fu F, Warner ME, Zhang Y, Feng Y, Hutchins DA (2007) Effects of increased temperature and CO₂ on photosyn-

- thesis, growth, and elemental ratios in marine *Synechococcus* and *Prochlorococcus* (Cyanobacteria). *J Phycol* 43:485–496
- Fu F, Mulholland MR, Garcia NS, Beck A and others (2008) Interactions between changing pCO₂, N₂ fixation, and Fe limitation in the marine unicellular cyanobacterium *Crocospaera*. *Limnol Oceanogr* 53:2472–2484
- Geider R, La Roche J (2002) Redfield revisited: variability of C:N:P in marine microalgae and its biochemical basis. *Eur J Phycol* 37:1–17
- Goericke R, Montoya JP (1998) Estimating the contribution of microalgal taxa to chlorophyll *a* in the field—variations of pigment ratios under nutrient- and light-limited growth. *Mar Ecol Prog Ser* 169:97–112
- Goldman JC, Peavey DG (1979) Steady-state growth and chemical composition of the marine chlorophyte *Dunaliella tertiolecta* in nitrogen-limited continuous cultures. *Appl Environ Microbiol* 38:894–901
- Hein M, Sand-Jensen K (1997) CO₂ increases oceanic primary production. *Nature* 388:526–527
- Hopkinson BM, Xu Y, Shi D, McGinn PJ, Morel FMM (2010) The effect of CO₂ on the photosynthetic physiology of phytoplankton in the Gulf of Alaska. *Limnol Oceanogr* 55:2011–2024
- Hopkinson BM, Dupont CL, Allen AE, Morel FMM (2011) Efficiency of the CO₂-concentrating mechanism of diatoms. *Proc Natl Acad Sci USA* 108:3830–3837
- Hutchins DA, Fu FX, Zhang Y, Warner ME and others (2007) CO₂ control of *Trichodesmium* N₂ fixation, photosynthesis, growth rates, and elemental ratios: implications for past, present, and future ocean biogeochemistry. *Limnol Oceanogr* 52:1293–1304
- Iglesias-Rodriguez MD, Halloran PR, Rickaby REM, Hall IR and others (2008) Phytoplankton calcification in a high-CO₂ world. *Science* 320:336–340
- Kim J, Lee K, Shin K, Kang J and others (2006) The effect of seawater CO₂ concentration on growth of a natural phytoplankton assemblage in a controlled mesocosm experiment. *Limnol Oceanogr* 51:1629–1636
- Kolber ZS, Prasil O, Falkowski PG (1998) Measurements of variable chlorophyll fluorescence using fast repetition rate techniques: defining methodology and experimental protocols. *BBA Bioenergetics* 1367:88–106
- Kranz SA, Sueltemeyer D, Richter K, Rost B (2009) Carbon acquisition by *Trichodesmium*: The effect of pCO₂ and diurnal changes. *Limnol Oceanogr* 54:548–559
- Landry MR, Ohman MD, Goericke R, Stukel MR, Tsyrlkevich K (2009) Lagrangian studies of phytoplankton growth and grazing relationships in a coastal upwelling ecosystem off Southern California. *Prog Oceanogr* 83: 208–216
- Laws EA, Bannister TT (1980) Nutrient-limited and light-limited growth of *Thalassiosira fluviatilis* in continuous culture, with implications for phytoplankton growth in the ocean. *Limnol Oceanogr* 25:457–473
- Leonardos N, Geider RJ (2005) Elevated atmospheric carbon dioxide increases organic carbon fixation by *Emiliania huxleyi* (Haptophyta), under nutrient-limited high-light conditions. *J Phycol* 41:1196–1203
- Levitan O, Rosenberg G, Setlik I, Setlikova E and others (2007) Elevated CO₂ enhances nitrogen fixation and growth in the marine cyanobacterium *Trichodesmium*. *Glob Change Biol* 13:531–538
- Lueker TJ, Dickson AG, Keeling CD (2000) Ocean pCO₂ calculated from dissolved inorganic carbon, alkalinity, and equations for K-1 and K-2: validation based on laboratory measurements of CO₂ in gas and seawater at equilibrium. *Mar Chem* 70:105–119
- McGinn PJ, Morel FMM (2008) Expression and regulation of carbonic anhydrases in the marine diatom *Thalassiosira pseudonana* and in natural phytoplankton assemblages from Great Bay, New Jersey. *Physiol Plant* 133:78–91
- Orcutt K, Lipschultz F, Gundersen K, Arimoto R, Michaels A, Knap A, Gallon J (2001) A seasonal study of the significance of N₂ fixation by *Trichodesmium* spp. at the Bermuda Atlantic Time-Series Study (BATS) site. *Deep-Sea Res Part II* 48:1583–1608
- Parkhill JP, Maillet G, Cullen JJ (2001) Fluorescence-based maximal quantum yield for PSII as a diagnostic of nutrient stress. *J Phycol* 37:517–529
- Parsons TR, Maita Y, Lalli CM (1984) A manual of chemical and biological methods for seawater analysis. Pergamon Press, Oxford
- Pickersgill RP (1986) An upper limit to the active-site concentration of ribulose biphosphate carboxylase in chloroplasts. *Biochem J* 236:311
- Raven J (1991) Physiology of inorganic C acquisition and implications for resource use efficiency by marine phytoplankton: relation to increased CO₂ and temperature. *Plant Cell Environ* 14:779–794
- Riebesell U, Wolgastrow DA, Smetacek V (1993) Carbon dioxide limitation of marine phytoplankton growth rates. *Nature* 361:249–251
- Riebesell U, Schulz KG, Bellerby RGJ, Botros M and others (2007) Enhanced biological carbon consumption in a high CO₂ ocean. *Nature* 450:545–548
- Rost B, Riebesell U, Burkhardt S, Sultemeyer D (2003) Carbon acquisition of bloom-forming marine phytoplankton. *Limnol Oceanogr* 48:55–67
- Shi D, Xu Y, Morel FMM (2009) Effects of the pH/pCO₂ control method on medium chemistry and phytoplankton growth. *Biogeosciences* 6:1199–1207
- Strickland JDH, Parsons TR (1972) A practical handbook of seawater analyses, 2nd edn. Fisheries Research Board of Canada, Ottawa
- Tortell PD, Rau GH, Morel FMM (2000) Inorganic carbon acquisition in coastal Pacific phytoplankton communities. *Limnol Oceanogr* 45:1485–1500
- Tortell PD, DiTullio GR, Sigman DM, Morel FMM (2002) CO₂ effects on taxonomic composition and nutrient utilization in an Equatorial Pacific phytoplankton assemblage. *Mar Ecol Prog Ser* 236:37–43
- Tortell PD, Payne C, Gueguen C, Strzepek RF, Boyd PW, Rost B (2008a) Inorganic carbon uptake by Southern Ocean phytoplankton. *Limnol Oceanogr* 53:1266–1278
- Tortell PD, Payne CD, Li Y, Trimbom S and others (2008b) CO₂ sensitivity of Southern Ocean phytoplankton. *Geophys Res Lett* 35, L04605, doi: 10.1029/2007GL032583
- Wang Z, Cai W (2004) Carbon dioxide degassing and inorganic carbon export from a marsh-dominated estuary (the Duplin River): a marsh CO₂ pump. *Limnol Oceanogr* 49:341–354
- Zhang H, Byrne R (1996) Spectrophotometric pH measurements of surface seawater at in-situ conditions: absorbance and protonation behavior of thymol blue. *Mar Chem* 52:17–25